Global characterization of protein secondary structures. Analysis of computer-modeled protein unfolding

G.A. Arteca,* O. Nilsson,† and O. Tapia†

**Department of Chemistry, University of Saskatchewan, Saskatoon, Saskatchewan, Canada, †Department of Physical Chemistry, University of Uppsala, Uppsala, Sweden*

Analyses of structural and molecular shape changes undergone by a protein during an unfolding process are presented. The procedure, based on a spherical shape map method, provides a topological description of a three-dimensional macromolecular structure. Local properties of the backbone are used to derive a global characterization of its fold. A spherical shape map of backbone crossings is associated with a given macromolecular conformation. The map is built by classifying each point on the sphere according to the crossing pattern obtained when the backbone is observed along a direction defined by the center of the sphere and the chosen point. The surface of the sphere can be divided in equivalence classes. All the points within a given class correspond to directions from which the backbone has the same overcrossing *pattern.*

Automatic computation and display of these equivalence classes is discussed, as is the implementation of the technique on a computer graphics workstation. The graphical manipulation simplifies the analysis of these maps when following a change in the conformation of the backbone. The procedure is illustrated with the results of a molecular dynamics computer simulation of the unfolding of the bacteriophage T4 glutaredoxin protein (in the form of its polyglycine model). The method gives a novel description of the differential structural stability for the characteristic secondary structural elements (α-helices and β-sheets) present in the protein. Recognition of the persistence of structural elements over the simulation time is performed in an unbiased manner.

Keywords: macromolecular shape, molecular dynamics, protein unfolding, shape fluctuations, structural stability

Color Plates for this article are on pages 189–190.

Address reprint requests to Dr. Arteca at his present address: Dept. of Chemistry and Biochemistry, Laurentian University, Ramsey Lake Road, Sudbury, Ontario P3E 2C6, Canada.

Received 7 October 1992; revised 18 January 1993; accepted 26 January 1993

INTRODUCTION

In this paper we apply a global description based on spherical maps of crossing patterns[1–3] to the study of secondary structure features in trajectories corresponding to a structural deformation (unfolding) process. This is an extension of the method previously used by us,[4] which allowed for a characterization of folds using crossing patterns found when viewing the structure along certain preferential directions in space.

Macromolecules are characterized by crossing patterns. These are found when viewing the system along certain preferential directions in space, and result from backbone segments overcrossing each other in space. From this pattern, a family of topological invariants is obtained describing some essential features of the protein's shape. These topological invariants can take the form of knot polynomials, associated with families of formal loops derived from the projected protein backbones.[1–3] A change in the view leads to a different planar projection, but not necessarily to a distinct topological description.

The previous computation introduces predefined directions in space, from which one explores the overcrossing pattern of the backbone.[1,4] The knot polynomials can be computed from these overcrossings. However, the ultimate choice of the directions is arbitrary. For this reason, one can resort to computing all the viewing directions. Theoretical foundations to this procedure have been developed recently.[3,5,6] The method uses the same information which is needed to construct the knot polynomials.

In this work we restrict ourselves to the use of spherical shape maps of overcrossing vectors (instead of knot polynomials), since they permit a greater discrimination between structures. The procedure is proposed as a tool to recognize different degrees of organization in a protein fold, as well as to make quantitative assessments on the persistence throughout the unfolding process of the various secondary structure features.

In the next sections we briefly describe the procedure and its application to the study of the dynamics of the unfolding of a polyglycine modeling the bacteriophage T4 glutaredoxin fold. The details on the computational implementation of the program on graphics workstations is given in the Appendix.

GRAPH—THEORETICAL CHARACTERIZATION OF MACROMOLECULAR BACKBONES

Consider the molecular backbone as a space curve, which can be expressed parametrically as:

$$\mathbf{r}(t) = x(t)\,\mathbf{i} + y(t)\,\mathbf{j} + z(t)\,\mathbf{k} \qquad 0 \leq t \leq 1 \tag{1}$$

where **i**, **j**, and **k** indicate the three unit vectors of an orthogonal Cartesian reference frame. The parameter t, varying from 0 to 1, defines the orientation of the backbone (from the N-terminal to the C-terminal).

For proteins, this curve is bounded and non-self-intersecting (disulfide bridges are ignored; see, however, Arteca et al.[4]). The segments exhibit an overcrossing (that is, two segments passing over one another) when viewed from a given direction in space. The number and type of overcrossings will change, up to a certain extent, with the viewing direction and with the changes in conformation of the backbone.

The crossing pattern provides essential topological information on the space curve. This information can be stored by means of vectors, whose dimensionality corresponds to the number of crossings, and whose elements are the crossing index (i.e., the handedness) of each crossing.[1-6] In turn, this information can be rendered into a simplified shape descriptor such as a knot type or a derived family of knot polynomials.[1,4]

The actual calculations are simply summarized here:[5]

(1) Consider the sequence of straight-line segments $\mathbf{r}(t)$. Enclose it completely by the smallest possible sphere S with origin at the geometrical center of the backbone.
(2) Pick a point on the sphere S. One can define a viewing direction **v** for the backbone between this point and the center of the sphere.
(3) When viewing the backbone from outside the sphere along the direction **v**, it is actually seen as a projection to a plane tangent to the sphere at the chosen point. Accordingly, a space curve with overcrossings is transformed into a planar curve with actual crossings.
(4) Now compute all the crossings within the planar curve and number them according to their order of occurrence when moving along the space curve.
(5) Each crossing can be given a *crossing index*, according to the handedness of the original overcrossing in the space curve. Right-handed overcrossings in 3-space are associated with a crossing index $C_i = 1$ for the ith crossing found from the given viewing direction. Similarly, a left-handed crossing has a corresponding crossing index $C_i = -1$.
(6) One can further characterize a crossing by the distance between the overcrossed segments. Using this value one can then focus the analysis on a selected subset of crossings, for example on those that satisfy the condition of occurring with distances below a desired cut-off value ϵ.[5]

As a result, the space curve can be characterized, for a given viewing direction **v**, by the vector **C** of crossing numbers:

$$\mathbf{C} = (C_1, C_2, \ldots C_m) \tag{2}$$

where m indicates the maximum number of crossings observed for the planar projection. Note that the curve will have exactly the same vector **C** for the viewing direction $-\mathbf{v}$. When the curve has no crossings for the given view, **C** cannot be defined. One can indicate formally this situation as $\mathbf{C} = 0$, without ambiguity.

The vector **C** is a *shape descriptor* for the curve at the chosen viewing direction. The procedure summarized above can be repeated for every direction **v** on the sphere, by a scanning procedure.

If one changes **v**, the shape description may or may not change. Points on the sphere S can then be classified into equivalence classes defined by having the same shape descriptor **C**. Accordingly, the sphere will exhibit "shape regions" where points share the same basic shape features, according to the present criterion. As a result, the shape characterization of a fold is transformed into the analysis of the shape regions on the sphere S. This display of shape regions on S is termed a *spherical shape map* (SSM).[5] It is the tool we apply in the next sections to the study of protein unfolding. Note that these maps have inversion symmetry.

The SSM provides a global three-dimensional (3D) characterization of the backbone. The approach uses local information on the curve, but leads to a global description, since the complete 3D nature of the protein is present in the final result (the equivalence classes of shape types on a sphere).

The procedure above is implemented in the computer program SPHERE.[7] The maps can be constructed by scanning the sphere S in a number of ways, and by focusing the attention on a certain shape type, for a given cut-off ϵ. Moreover, the maps can be displayed and manipulated by the graphical program SHAPES[8] for the Silicon Graphics workstations. The main features of these programs are discussed in the Appendix. In the next section we comment on the SSMs for some characteristic secondary structural elements of proteins, and their changes over time.

SECONDARY STRUCTURE CHARACTERIZATION

A great deal of effort has been done regarding the behavior of helices when the protein undergoes significant structural changes.[9-12] Under certain conditions, helices seem to remain rigid, thus being replaceable by simplified structures such as their axes or cylinders.[13] However, under different conditions helices may be completely unfolded.

The SSM method has the attractive feature of providing "fingerprint" maps which are characteristic of helices and strands.[5] In Arteca and Mezey[5] an analysis is given of the SSMs for basic secondary structural features. In Arteca,[6] the work was extended to the case of helical bundles. It is important to summarize here the findings, since they are an essential result for the discussion that follows. The properties discussed below are illustrated in the figures in the following section.

(1) Consider an ideal, perfectly cylindrical α-helix. The helix shows the larger number of overcrossings when observed along directions closer to the helical axis. On the other hand, directions which form angles closer to 90° with the axis do not show overcrossings. Accordingly, if one pays attention only to the equivalence

class of directions with shape type $\mathbf{C} = 0$, a helix presents a no-crossing region which is a "band" at the spherical equator (when the "poles" are aligned with the helical axis).

(2) The extension of the central region of no-crossings depends on the length of the helix. Shorter cylindrical helices have wider no-crossing bands. Moreover, if the helix is short enough (typically seven residues or less) there are two small, disconnected no-crossing regions close to the poles.

(3) The shape and extension of this region depends on the degree of deformation of the actual structure away from an ideal cylindrical helix. Uneven stretchings in the helix lead to the narrowing of the no-crossing region. In a further distortion, the helix can become *stacked*. In this case, each loop is formed by atoms occupying almost coplanar positions, and every loop is connected by segments almost perpendicular to it. In this case, the no-crossing band tends to break symmetrically into two disjoint regions (a further step from the above narrowing).

(4) Bending a helix also breaks the central band feature, but in a less symmetrical manner.

(5) From the point of view of the no-crossing band, a β-sheet appears almost as a complementary object to the α-helices. When a sheet is observed from direction close to its plane, it exhibits a larger number of crossings. By contrast, directions perpendicular to the plane will not exhibit overcrossings since the β-strands will appear approximately parallel to each other. As a result, the SSM shows crossings only in a narrow equatorial region.

(6) If a structure unfolds completely into an open strand, then the SSM will show crossings for very few regions of space. In this case, the $\mathbf{C} = 0$ equivalence class fills almost the whole sphere.

These features provide a simple characterization of standard elements of secondary structure. Real cases can be classified, in principle, as belonging to some of these ideal cases or as being derived from them by some distortion.

So far we have described structures according to their $\mathbf{C} = 0$ spherical shape maps. These maps provide simply a strategy to explore the shape features of the backbone. There is no loss of generality in the approach, and any other shape types or number of crossings can be explored. The analysis of the maximum number of crossings, instead of the no-crossing band, provides also a good deal of information. However, the determination of the maximum number of crossings is a variational problem having a quite difficult solution. Instead, one can simply resort to analyze the regions with many crossings, the latter being specified by all the regions which have crossings larger than a given lower bound to m.

In the next section we apply these ideas to the results of a computer-modeled unfolding of glutaredoxin.

GRAPHICS ANALYSIS OF A MODEL BACTERIOPHAGE T4 GLUTAREDOXIN UNFOLDING

The chosen protein, bacteriophage T4 glutaredoxin (T4glx), is a redox active, α/β type of protein with 87 amino acid residues.[14,15] It consists of two folding units. The first one, spanning residues 1–49, has a $\beta\alpha\beta$ structure, and it is connected through two loops and a helix to the second unit (residues 50–87) which contains a $\beta\beta\alpha$ structure. The molecule contains a four-stranded β-sheet, and three helices. The helices are different in length. Helix α_1 has 13 residues, α_2 has 10, and α_3 only 7.

A number of molecular dynamics studies have been performed for this protein.[16–19] Of all those, we shall concentrate on the simulations of T4glx by means of a polyglycine model. Two simulations are analyzed. In one case all the electrostatic terms of the interaction are removed. This rapidly makes the system unstable over time, allowing one to observe marked structural transitions within relatively short simulations. In the other case, all electrostatic contributions are fully considered, making the unfolding of the system much slower.

Simulation With No Electrostatic Effects

In this case the system presents very rapid unfolding changes within the first 6.0 ps. The analysis of this first step has been carried out in two stages. First, we examine the evolution of the helical segments; second, we explore the remaining of the backbone when the helices are removed.

Color Plates 1–3 illustrate sequences of spherical shape maps found every 1.0 ps for helices α_1, α_2, and α_3, respectively. The maps (displayed with the program SHAPES) show the no-crossing, $\mathbf{C} = 0$, in dark. Hues of color are used to give an impression of 3D depth. The ruggedness in the boundaries of the regions is due to the numerical scanning of points on the sphere. In all the cases studied in this work we have employed a 3° scanning in both spherical angles θ and ϕ.

The initial point corresponds to a conformation 0.1 ps away from the starting X-ray structure. The spherical shape maps at 0.1 ps reveal clearly that we have three normal helices. The fact of α_3 being the shorter one is manifested in the width of its central band and in the presence of two small no-crossing caps near the poles. In all cases, the backbone structure has been displayed as well inside the sphere for the sake of clarity.

The helices have quite different behavior when the system evolves. Color Plate 1 shows that helix α_1 oscillates between a normal helix and a stacked one up to 2.1 ps. After this, the SSM suggests the occurrence of more extensive distortion away from the normal helix, but without destroying all the helical features. In contrast, helix α_2 presents very small distortions from the typical 'central band' of no-crossings (Color Plate 2). As far as the analysis is concerned, the second helix is preserved during the early stages of the simulation. Finally, helix α_3 (Color Plate 3) is distorted completely from the beginning of the simulation. Note that the maps for 3.1 ps and 4.1 ps are almost fully covered. This is a feature characteristic of β-sheets. This is an indication that the helix has unfolded entirely and bent, resembling now a sort of "short sheet" with two strands.

The SSMs shown in Color Plates 1–3 illustrate some of the typical changes found for conformations along the molecular dynamics simulation. The detailed study of the whole path would require one to monitor shape invariance

maps for a large number of conformations. However, we can resort to a simplified analysis. There are two features of importance in a no-crossing map for helices. One of them is the area of the no-crossing region and the other is the number of disjoint sets (maximum connected components) in it. The number of disjoint regions presents a measure of change from a standard structure. The area on the sphere S gives an idea of the extent of the distortion (for instance, areas will be larger when unfolding a stacked helix into a series of strands).

The results of this 'condensed' analysis are shown in Figures 1–3 for the helices α_1, α_2, and α_3, respectively. These diagrams reveal immediately the evolution of the helices along the folding path. Note that all three diagrams start from a value of 0.32 to 0.35 for the area (measured as fraction of the sphere's surface). This value of area appears to be a characteristic of a helix.[6]

Consider first Figure 1. The area for a single region (normal helix band) is approximately constant up to 1.1 ps. At this point the region becomes disconnected. When the region unites again, it does so with a decrease in area over time. This indicates that the helix is being deformed, probably by elongation. Between 3.0 ps and 4.0 ps the no-crossing band breaks into pieces, coinciding with an increase in the area. This is a clear indication of the structure becoming unfolded into open strands. At this moment, one could assess that the former helix is entering another structural regime. According to the topological criterion we follow here, one would no longer describe it as a helix. Observe, however, that the change is not permanent, as the structure becomes helical again at about 4.5 ps. The system does not become unfolded in a single thrust. There is an oscillation from helix to open strands, and the method allows one to recognize the extent of these motions.

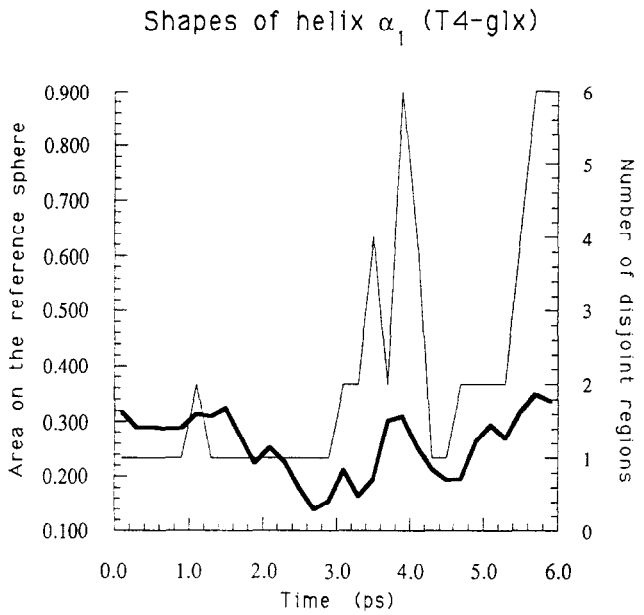

Figure 1. Area (thick line) and number of no-crossing regions (thin line) for the α_1 helix of T4glx as a function of time. No electrostatic terms are included in the simulation. The area is expressed as a fraction of the total area of the sphere S.

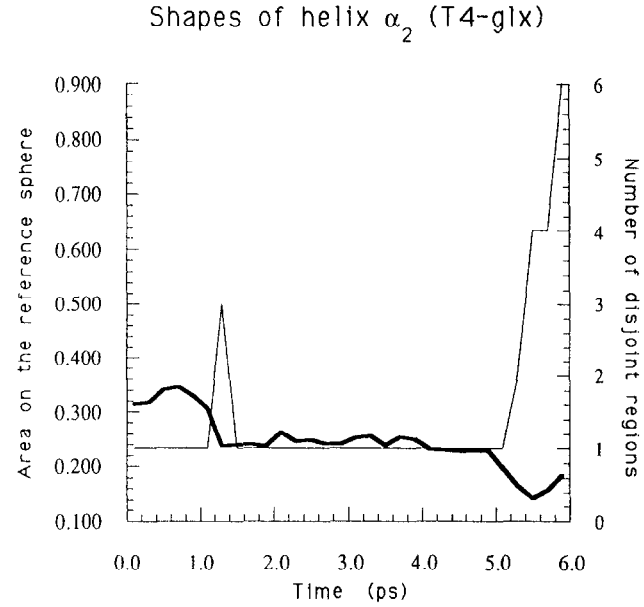

Figure 2. Area (thick line) and number of no-crossing regions (thin line) for the α_2 helix of T4glx as a function of time. No electrostatic terms are included in the simulation. The area is expressed as a fraction of the total area of the sphere S.

Figure 2 shows the results for helix α_2. Note that the perfect helix survives up to 1.3 ps, where it becomes elongated (partly stacked). After this, it remains basically unchanged as a helix, up to 5.0 ps where a new distortion can be observed. It is clear that this helix is more rigid than α_1.

Figure 3 shows a completely different behavior for the

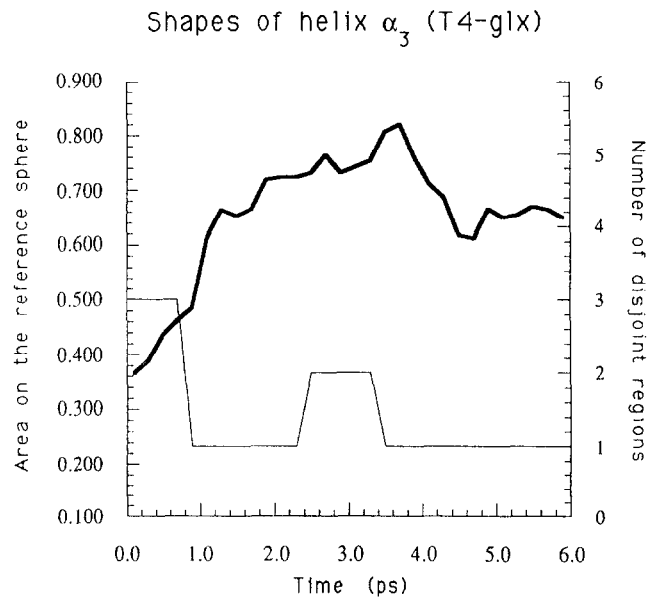

Figure 3. Area (thick line) and number of no-crossing regions (thin line) for the α_3 helix of T4glx as a function of time. No electrostatic terms are included in the simulation. The area is expressed as a fraction of the total area of the sphere S.

shorter helix α_3. The starting structure has a no-crossing region made up of three disjoint pieces (as expected). However, at 0.9 ps this region collapses into a single one and the area increases rapidly with time. This sudden change indicates a distortion from helix to an object which does not present many overcrossings. This is characteristic of a turn, or of two almost parallel strands. The results indicate immediately that this helix is the most elastic, becoming completely unfolded at about 1.0 ps.

If the system is allowed to evolve for a longer time, finally all helices disappear. We have computed this trajectory without electrostatic contributions up to 100 ps. As an illustration, Color Plate 4 shows the SSM for the three helices at 90 ps. Note the absence of no-crossing bands. On the contrary, the maps for the three helices have large disconnected no-crossing caps. As mentioned in the previous section, this is a characteristic of systems resembling planes of strands. One can conclude that the three helices have disappeared as such, being unfolded up to different degrees. Helices α_1 and α_2 have become loose, open loops. By contrast, the former helix α_3 appears now as an extreme example of a structure with two short, almost coplanar strands.

This analysis has been restricted to the helices. The procedure can be applied in a similar manner to the whole backbone or the two folding units. However, the more complicated the structure, the larger the number of overcrossings it has. As a matter of fact, the spherical shape maps may not show any no-crossing region whatsoever.[20] Taking into account this possibility, we suggest the following strategy to the analysis of the remaining features of the fold: First, replace the helices (whose behavior has already been analyzed) by straight-line segments. Then, analyze the overcrossing pattern of the backbone for different cut-off values. This ensures that the sphere will display regions with and without crossings, allowing the identification of the loosely and densely packed regions of the fold.[5]

Color Plate 5 shows the results of applying above procedure to the initial structure (at 0.1 ps). If no cut-off is introduced, then the backbone overcrosses itself from all directions in space. Accordingly, when a cut-off distance ϵ is introduced, then all crossings with distance larger than or equal to ϵ are ignored. These directions will then become no-crossing regions.

We have used decreasing values of ϵ from 6.0 Å down to 4.0 Å. At the largest value, only very few crossings are ignored. Observe that when the value of ϵ decreases, the crossings ignored occupy a ring around the structure. The section of the backbone pointing towards the reader corresponds to the core of the β-sheet, and it is always open. This region has a high number of overcrossings; i.e., it is a structure with a rather compact packing of α-carbons. It must be kept in mind that the studied object is a polyglycine model, thus the absence of side chains may artificially permit unusually short distances between backbone atoms.

Color Plate 6 complements the analysis by showing the same views at 5.9 ps. It can be immediately noted that there is an overall shift of features towards the shorter distances. In this case it is necessary to go up to cut-off values as low as 3.4 Å to obtain a structure comparable to that for 4.0 Å at 0.1 ps. Nevertheless, the shape of the map still suggests the persistence of a β-sheet as a feature, though distorted and with the central atoms squeezed together.

Simulation Including All Electrostatic Effects

The inclusion of electrostatic terms keeps the backbone together for a longer time preventing unfolding. The changes that could be seen in the previous model at a few picoseconds take longer in this case.

We have performed exactly the same type of analysis for the three helices. The summary is given in Figures 4–6, which indicate areas on the sphere S and the number of disjoint regions for the no-crossing equivalence classes for helices α_1, α_2, and α_3, respectively. The results correspond to a simulation up to 300 ps. Note that the time scale is logarithmic in this case. The initial structure corresponds to 1.0 ps.

An analysis of Figures 4–6 shows a few interesting differences in the evolution of the α-helices when compared with the previous approach. First of all, helix α_1 is preserved as such during the whole trajectory (Figure 4). Note that we have always a characteristic no-crossing band, with modest oscillations in area. We can state that the helix undergoes regular elongations (which reduce the area of the $\mathbf{C} = 0$ region), but it keeps a helical structure all the way. Color Plate 7 reinforces part of the analysis by showing some characteristic maps found along the trajectory. The map for 9.0 ps corresponds to the absolute minimum in area (Figure 4). Here it would appear that the distortion on the helix is a combination of stretching and bending.

Figure 5 shows the results for helix α_2. A number of selected maps appear in Color Plate 8. The diagram shows

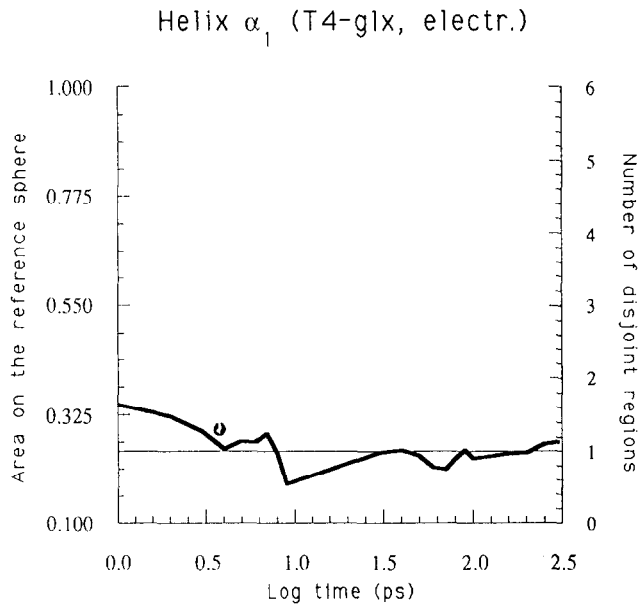

Figure 4. Area (thick line) and number of no-crossing regions (thin line) for the α_1 helix of T4glx as a function of time. All electrostatic terms are included in the simulation. The area is expressed as a fraction of the total area of the sphere S. Note that the timescale is logarithmic, spanning from 1 ps to 300 ps.

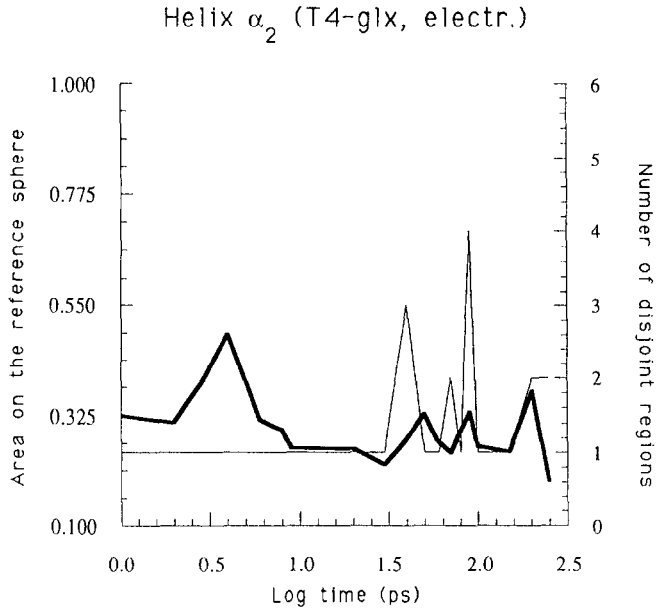

Figure 5. Area (thick line) and number of no-crossing regions (thin line) for the α_2 helix of T4glx as a function of time. All electrostatic terms are included in the simulation. The area is expressed as a fraction of the total area of the sphere S. *Note that the timescale is logarithmic, spanning from 1 ps to 300 ps.*

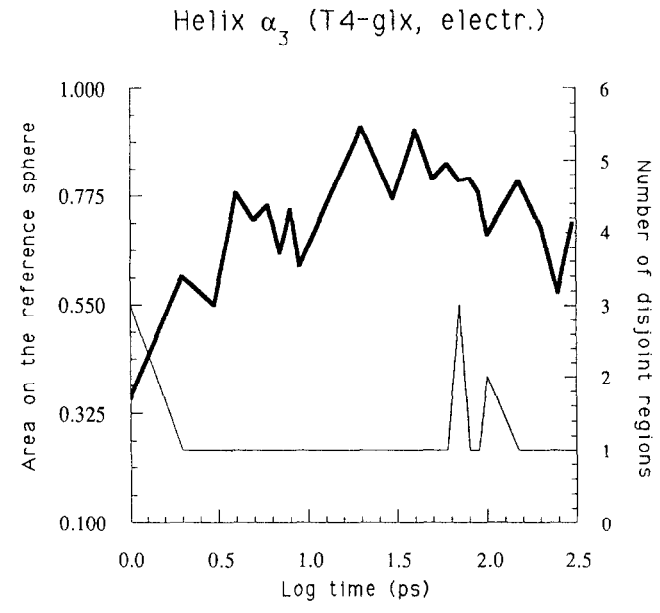

Figure 6. Area (thick line) and number of no-crossing regions (thin line) for the α_3 helix of T4glx as a function of time. All electrostatic terms are included in the simulation. The area is expressed as a fraction of the total area of the sphere S. *Note that the timescale is logarithmic, spanning from 1 ps to 300 ps.*

that this helix is not preserved as such during the whole path. One can recognize several regimes. One of them, up to 3.5 ps (0.55 in log time in Figure 5), can be described as a distorted helix. Another regime lies between 9.0 ps and 31.0 ps, in which the system is partly unfolded. In this case we find features of a helix, such as a single connected no-crossing region with the correct value of the area. However, the "shape" of the region is not a band. The shape suggests a helix, of which only a section has unfolded. From 31 ps to 100 ps the structure passes to another situation, further unfolded.

Finally, Figure 6 and Color Plate 9 show the results for the shorter helix α_3. As was found in the case of ignoring the electrostatic terms, this helix is very flexible. Figure 6 shows again a rapid increase in the area of the no-crossing region, indicating the occurrence of an open structure with nearly coplanar strands. From our results, we cannot talk any longer of a helix after approximately 2.0 ps. Between 10 ps and 60 ps, approximately, the structure remains as two almost coplanar strands (a horseshoe).

These latter results are qualitatively the same, whether including or not the electrostatic contributions. On the other hand, the behavior of helices α_1 and α_2 seems reversed. The former is preserved when including electrostatic contributions, whereas the latter is rigid in the short time window of the simulation without electrostatic terms. The differences in the helices' behavior in the two polyglycine simulations may be rationalized by considering the differences in their 3D environments.

FINAL COMMENTS AND CONCLUSIONS

The SSM method has been shown to provide an insight into the recognition of *shape persistence* in the folding or unfolding of a backbone. The technique can be implemented to explore a whole backbone (provided that appropriate cut-offs are introduced to monitor crossings) or just a section of it.

The procedure allows location of shape transitions (that is, the topological equivalent to structural transitions) along a molecular dynamics trajectory.[20] Degrees of distortion can be sensed. It is possible to distinguish the effects of small amplitude vibrations on a helix (elongations and bending) from those changes leading to partial or complete unfolding of the helical loops. Both situations can be differentiated as they lead to different crossing patterns.

It is worth noting that there are other procedures used in the literature to monitor shape transitions. For example, one can study the changes in local principal moments of inertia of a helical section along the trajectory.[17-19] As in the SSM method, the input is geometrical. However, the procedure applied in this work produces a *global* description built from *local* geometrical properties. Note that one does not associate one number (or three in the case of the principal moments of the inertia tensor) with a conformation, but a map of spherical projections. This map contains all the possible views of the object, and thus fully provides a description of the essential 3D shape features.

Two numbers, the area of the no-crossing region and its number of maximum connected pieces, seem to retain some of the important properties of the SSMs. In this manner one can follow the evolution of structural features by means of

single-variable functions, which simplifies the analysis.[6,20] In principle, a similar one-variable measure can be developed for the analysis of full backbones using cut-offs. One can describe, for instance, the area of the no-crossing region or the maximum number of crossings as a function of the cut-off value. This would provide a simple function, instead of a 3D map, to characterize the backbone's shape features. This possibility, as well as the role of the higher order crossing, will be explored when studying other molecular dynamics trajectories.

ACKNOWLEDGMENTS

GAA acknowledges inspiring discussions with Profs. P.G. Mezey and R. Somorjai on molecular space curves. This work has been supported by grants from NSERC (Canada) and NFR (Sweden).

APPENDIX

The algorithm for shape characterization of molecular backbones is implemented in a FORTRAN program SPHERE. The actual display and 3D manipulation of the spherical shape maps is performed by the graphics program SHAPES, for the Silicon Graphics workstations.

The features of these programs are as follows:

(1) SPHERE allows the interactive exploration of any given desired direction of space or the automatic computation of the total spherical shape map. Directions can be specified as either spherical angles or in vector form. Computations are fast and accurate, as all the equations are solved analytically. The construction of the spherical maps, by contrast, is performed with a user-defined accuracy for scanning the sphere according to the spherical angles θ and ϕ.

(2) SPHERE constructs spherical maps for any desired shape type. Shape types can be specified by the full crossing vectors **C**, or simply by the total number of crossings, disregarding the handedness. Cut-off values can be defined as desired.

(3) SHAPES is a graphic facility for interpreting the output of SPHERE. The program allows the displaying of the spherical shape maps in 3-space or in two-dimensional projections. The display can be modified through a number of pop-up menu options.

(4) SHAPES permits the presentation of spherical maps as dot surfaces or solid surfaces, with illumination. The option of coloring the maps according to the shape types is included. Real-time rotation of the spheres, resizing, and stereo (3D) display are also available.

REFERENCES

1 Arteca, G.A. and Mezey, P.G. *J. Mol. Graph.* 1990, **8,** 66
2 Arteca, G.A. and Mezey, P.G. In: *Computational Chemistry: Structure, Interactions, and Reactivity.* (S. Fraga, Ed.) Elsevier, Amsterdam, 1992
3 Arteca, G.A. and Mezey, P.G. In: *Theoretical and Computational Models for Organic Chemistry.* (S.J. Formosinho, I.G. Csizmadia, and L.G. Arnaut, Eds.) NATO ASI, Kluwer, Dordrecht, 1991
4 Arteca, G.A., Tapia, O., and Mezey, P.G. *J. Mol. Graph.* 1991, **9,** 148
5 Arteca, G.A. and Mezey, P.G. *Biopolymers* 1992, **32,** 1609
6 Arteca, G.A. *J. Math. Chem.* 1993, **12,** 37
7 Arteca, G.A. Program SPHERE, 1991, University of Saskatchewan
8 Nilsson, O. and Arteca, G.A. Program SHAPES, 1991, University of Uppsala and University of Saskatchewan
9 Chothia, C., Lesk, A.M., Dodson, G.C., and Hodkin, D.C. *Nature* 1983, **302,** 500
10 Lesk, A.M. and Chothia, C. *J. Mol. Biol.* 1985, **174,** 175
11 Lesk, A.M. and Chothia, C. *J. Mol. Biol.* 1980, **136,** 225
12 Chothia, C. and Lesk, A.M. *J. Mol. Biol.* 1985, **182,** 151
13 Rojewska, D. and Elber, R. *Proteins* 1990, **7,** 265
14 Söderberg, B.-O., Sjöberg, B.M., Sonnerstam, U., and Brändén, C.-I. *Proc. Natl. Acad. Sci. USA* 1978, **75,** 5827
15 Eklund, H., Ingelman, M., Söderberg, B.-O., Ulin, T., Nordlund, P., Nikkola, M., and Joelsson, T. *J. Mol. Biol.* 1992, **228,** 596
16 Nilsson, O., Tapia, O., and van Gunsteren, W.F. *Biochem. Biophys. Res. Comm.* 1990, **171,** 581
17 Tapia, O. and Nilsson, O. In: *Molecular aspects of biotechnology: Computational models and theories.* (J. Bertran, Ed.) NATO ASI, Series C, **368** pp. 123–152, Kluwer, Dordrecht, 1992
18 Nilsson, O. Ph.D. Thesis, University of Stockholm, 1991
19 Nilsson, O. and Tapia, O. *J. Mol. Struct. (Theochem)* 1992, **256,** 295
20 Arteca, G.A. *J. Comp. Chem.* 1993, **14,** 718